Egyptian Journal of Radiology and Nuclear Medicine

RESEARCH

Open Access

Glioma grading using an optimized T1-weighted dynamic contrast-enhanced magnetic resonance imaging paradigm

Aza Ismail Abdi[1,2*]

Abstract

Background Glioma grading is a critical procedure for selecting the most effective treatment policy. Biopsy result is the gold standard method for glioma grading, but inherent sampling errors in the biopsy procedure could lead to tumor misclassification.

Aim This study evaluated grading performances of a more comprehensive collection of the physiological indices quantified using an optimized dynamic contrast-enhanced magnetic resonance imaging (DCE-MRI) paradigm for glioma grading.

Methods Thirty-five patients with glioma underwent DCE-MR imaging to evaluate the grading performances of DCE-MRI-derived physiological indices. The statistical differences in the physiological indices between the different grades of gliomas were studied, and the grading performances of these parameters were evaluated using the leave-one-out cross-validation method.

Results There were significant statistical differences in DCE-MRI-derived physiological indices between the different grades of gliomas. The mean rCBVs for grade II (low-grade glioma, LGG), grade III, grade IV, and high-grade (HGG) gliomas were 2.03 ± 0.78, 3.61 ± 1.64, 7.14 ± 3.19, and 5.28 ± 3.02, respectively. The mean rCBFs of 1.94 ± 0.97, 2.67 ± 0.96, 4.57 ± 1.77, and 3.57 ± 1.68 were, respectively, quantified for grade II (LGG), grade III, grade IV, and high-grade gliomas. The leave-one-out cross-validation method indicates that the grades of glioma tumors could be determined based on a specific threshold for each physiological index; for example, the optimal cutoff values for rCBF, rCBV, Ktrans, Kep, and Vp indices to distinguish between HGGs and LGGs were 2.11, 2.80, 0.025 mL/g min, 0.29 min^{-1}, and 0.065 mL/g, respectively.

Conclusions From the results, it could be concluded that glioma grades could be determined using DCE-MRI-derived physiological indices with an acceptable agreement with histopathological results.

Keywords Glioma grading, Dynamic contrast-enhanced MRI, Cerebral hemodynamic indices, Permeability indices, Perfusion-weighted MRI

Background

Gliomas are the most common primary cerebral neoplasms which are categorized as highly vascularized malignant tumors [1–4]. More than half of all brain tumors in patients are gliomas, approximately 53% [5]. Brain tumors are classified according to their morphological, immunochemical, and molecular characteristics. In the World Health Organization (WHO) classification

*Correspondence:
Aza Ismail Abdi
aza.ismael@epu.edu.iq
[1] Department of Radiology, Erbil Medical Technical Institute, Erbil Polytechnic University, Erbil, Iraq
[2] Medical Technical College, Al-Kitab University, Kirkuk, Iraq

criteria, tumors are assigned a grade based on the histopathological features and immunohistochemical evaluations [6, 7].

Glioma grading is a critical procedure in selecting the most effective therapy policy. High-grade gliomas are usually treated by adjuvant radiation therapy and chemotherapy (after surgery) with a more aggressive treatment plan, whereas low-grade glioma would be differently treated [8].

Biopsy results are the gold standard method for glioma grading, but inherent sampling errors in the biopsy procedure could lead to tumor misclassification [9–11]. Gliomas are typically heterogeneous. If the biopsy sites are not properly selected or the biopsy samples have been too small, a lower grade might be assigned to the tumor. These erroneously assignments lead to selecting a non-optimal therapeutic strategy [12, 13]. There is an increasing interest in other complementary techniques such as imaging approaches. The magnetic resonance imaging (MRI) method is the most common imaging modality in the evaluation of brain tumors. Conventional MRI techniques have inherent limitations in evaluating the proliferation potential of the tumors [14, 15]. Advanced MRI methods are required to investigate the microvascular, angiogenesis, metabolism, micronecrosis, and cellularity characteristics of tumors. The bio-imaging markers can provide valuable supplementary information for glioma grading [13]. Recently, several sophisticated MRI techniques have been introduced that allow assessing the metabolic and physiological characteristics of the brain tissues [14, 16].

The perfusion weighted-magnetic resonance imaging (PW-MRI) method is one of the clinically most relevant procedures of functional MRI, which is used to assess microvasculatures, neovascularization, and capillary permeability of tumors. The assessment of tumor hemodynamics (including blood flow, blood volume, and vessel permeability) could give considerable insight into the angiogenic process of the tumor and provide additional pathological information for preoperative glioma grading [3, 17].

Tumor neo-angiogenesis results in tortuous and leaky vessels due to the lack of muscularis propria, widened interendothelial junctions, and a discontinuous or absent basement membrane. Therefore, the permeability of tumor microvasculature would significantly increase. The permeability indices describe the predominant characteristics of tumor vessels [18]. Physiological characteristics of the tumors including microvascular proliferation, aggressive cellular characteristics, and tumor-induced angiogenesis could be indirectly evaluated using perfusion indices [19].

The cerebral hemodynamic and permeability parameters are currently quantified using dynamic susceptibility contrast MRI (DSC-MRI) and dynamic contrast-enhanced MRI (DCE-MRI) approaches, respectively. Pioneer studies have shown that cerebral hemodynamic indices could be accurately quantified using an optimized DCE-MRI paradigm [20–22]. Quantification of tumor hemodynamics (including cerebral hemodynamic and permeability indices) based on single-dose imaging would be a useful alternative approach for tumor assessments, taking into account the cost of double-dose acquisitions and patient safety issues. This study employs an optimized DCE-MRI-based paradigm to quantify cerebral hemodynamic and permeability indices in gliomas and evaluates the performance of the extracted parameters for glioma grading.

Methods

Imaging protocols

MRI scans were performed on a 1.5-Tesla clinical MRI scanner (Magnetom Avanto, Siemens Medical Solutions, Erlangen, Germany). The MRI protocols included axial pre- and post-contrast T1-weighted spin-echo (TR/TE = 370/8.7 ms; flip angle = 90; slice thickness = 5 mm; NEX = 1; matrix = 512 × 464) and transverse T2-weighted spin-echo (TR/TE = 3300/99 ms; echo train length = 11; flip angle = 120; slice thickness = 5 mm; NEX = 2; matrix = 384 × 288) sequences. Variable flip angle technique(VFA) was used for T1 mapping, which employs a gradient echo sequence with different flip angles (α = 2°,10°,20°, and 25°; TR = 12 ms; TE = 3.5 ms; matrix size = 256 × 224; NEX = 1; slice thickness = 5 mm).

The gradient-recalled echo sequence (GR) was used for T1W DCE-MR imaging. The scanning parameters applied for perfusion imaging were: TR = 4.13 ms, TE = 1.54 ms, field of view = 200 × 200 mm2, matrix size = 256 × 224, flip angle = 15°, NEX = 1, slice thickness = 5 mm, number of measurements = 70, and gap = 5 mm.

DCE-MR images were obtained following the administration of gadoteric acid (Dotarem; Guerbet, Paris, France) in a dose of 0.1 mL/kg body weight. The injection was performed using an automatic injector at a rate of 2mL/ second followed by a 15 mL saline flush at the same rate.

DCE-MRI analysis

Motion correction of DCE-MR images was performed using the MCFLIRT function in the FMRIB Software Library (FSL; University of Oxford: http://www.fmrib.ox.ac.uk/fsl/). A 3 × 3 mean filter was used for data smoothing, and brain extraction was performed using a

semi-automatic MATLAB-based program (ver. 2008a, The MathWorks TM, Natick, Massachusetts, United States).

T1W DCE-MRI data were analyzed using in-house-developed perfusion software (based on MATLAB software). The permeability indices were quantified based on the modified Kety-Tofts model. The ROIs were determined by a mouse pointer-aided method. For each physiological index, the mean values of the ROIs were registered.

Semi-quantitative analysis

Semi-quantitative indices including the initial area under the curve (IAUC60(mmol/L*Sec)), the peak contrast enhancement (Peak (mmol/L)), and the slope of the time-contrast enhancement curve (Wash-in rate (mmol/L/Sec)) are quantified using the time-contrast concentration curve. IAUC index is a robust estimation for tissue vascularization [23–25].

The area under the time-contrast enhancement curve from the time point of the contrast uptake to 60 s after the onset time was considered as the IAUC60. The trapezoidal method was used for the IAUC60 calculation. The peak is the absolute maximum contrast enhancement for the time-contrast concentration curve. The wash-in rate is the slope of the best-fitted line from the contrast uptake to 10 s after the onset time. The wash-in rate was determined by the sum-of-least-squares method.

Quantification of CBV and CBF indices based on the DCE-MRI data

Cerebral blood volume (CBV) and cerebral blood flow (CBF) indices could be determined based on the T1W DCE-MRI data with good agreement with the DSC-MRI-derived cerebral hemodynamic indices [22]. In this study, cerebral hemodynamic indices were quantified based on the DCE-MRI using a validated method [20, 22, 26]. Cerebral blood volume (CBV) was measured using Eq. 1:

$$\mathrm{CBV}_{\mathrm{Uncorrected}} = \frac{H}{\rho}\frac{\int C(t)dt}{\int C_a(t)dt} \tag{1}$$

where $C(t)$ and $C_a(t)$ are the arterial and tissue time–concentration curves, ρ is the brain tissue density (1.04 g/mL), and $H=(1-\mathrm{Hart})/(1-\mathrm{Hcap})$ was applied to differentiate capillary hematocrits (Hcap = 25%) from large vessel hematocrits (Har = 45%).

CBV is the blood volume of the intravascular space. The blood volume of the leakage space has been reported as a part of the CBVuncorrected. Therefore, CBVuncorrected was corrected by the removal of volume contribution of fractional leakage space (Ve) as:

$$\mathrm{CBV\ corrected} = \mathrm{CBV}_{\mathrm{uncorrected}} - \mathrm{veCBV}_{\mathrm{uncorrected}} \tag{2}$$

CBF index (in mL/100gr.min) was quantified using the following equation:

$$\mathrm{CBF}.R = \frac{1}{\rho.H}F^{-1}\left\{\frac{F\{C(t)\}}{F\{\mathrm{Ca}(t)\}}\right\} \tag{3}$$

where R is the residual function, and $\mathrm{F}-1\{\}$ denotes the inverse Fourier transformation.

Patients

Thirty-five patients diagnosed with glioma underwent DCE-MR imaging to assess the performance of DCE-MRI-derived physiological indices for glioma grading. Patients were selected from individuals seeking medical oncologist consultations at Erbil Teaching Hospital. Prior to their participation in the study, informed consent was obtained from all patients. The patients were scanned before any medical interventions, and their glioma grades were determined based on the biopsy results. The demographic information of the patients is summarized in Table 1. The study was approved by the local committee for medical research ethics.

Patients' data were analyzed using the mentioned algorithms and methods in the previous section. For each patient, the region of interest (ROI) was selected on the high perfusion area of the CBV map [27]. The relative cerebral hemodynamic changes (rCBV and rCBF) were measured as the mean cerebral hemodynamic magnitude of tumor ROI divided by the mean value in the mirror ROI on the contralateral normal lobe.

Statistical analysis

The normality of the distribution of DCE-MRI-derived physiological indices was checked using the Shapiro–Wilk test. The *Mann–Whitney* U *test* and independent student T test analyses were used to evaluate the difference in the parameters between the different grades of gliomas.

Evaluation of DCE-MRI-derived physiological indices for glioma grading

In classification studies, cross-validation methods are used to achieve an optimal classifier. In this method, different classification structures are examined and the classification performances of these structures would be determined. Finally, the classification structure with the best classification performance is chosen. The results of these methods are not reliable when the study sample size is small. The leave-one-out cross-validation method could yield reliable results in such cases. In this study, the leave-one-out cross-validation method is used to

Table 1 Demographic and clinical characteristics of the studied patients

Patient no	Sex	Age	Tumor type
1	M	27	Oligodendroglioma (II)
2	F	41	Oligoastrocytoma (II)
3	M	24	Oligodendroglial (III)
4	M	43	Oligodendroglioma (II)
5	M	23	Astrocytoma (II)
6	F	38	Astrocytoma (II)
7	M	50	Anaplastic Oligodendroglioma (III)
8	M	25	Diffuse Astrocytoma (III)
9	M	29	Fibrillary astrocytoma with areas of anaplastic transformation according to WHO(II-III)-(III)
10	F	35	Oligodendroglial(III)
11	M	46	GBM (IV)
12	M	36	Anaplastic Oligodendroglioma (III)
13	F	31	Oligoastrocytoma (II)
14	M	27	Diffuse astrocytoma (II)
15	M	29	Low grade glioma -astrocytoma (II)
16	M	66	Astrocytoma Anaplastic(III)
17	M	35	Oligodendroglioma (II)
18	M	28	Oligoastrocytoma (II)
19	M	41	Gemistocytic astrocytoma with anaplastic transformation (III)
20	F	28	Oligodendroglioma (II)
21	F	38	GBM(IV)
22	M	24	Oligodendroglioma (II)
23	M	56	Oligoastrocytoma (II)
24	M	35	Oligodendroglioma with microcystic component (II)
25	F	39	Oligodendroglioma (III)
26	F	30	Anaplastic astrocytoma (III)
27	M	28	Oligoastrocytoma (II)
28	F	57	GBM (IV)
29	F	36	Oligoastrocytoma (II)
30	F	35	GBM(IV)
31	F	21	GBM(IV)
32	F	78	GBM(IV)
33	M	67	GBM(IV)
34	F	45	GBM(IV)
35	F	49	GBM(IV)

evaluate the grading performances of DCE-MRI-derived physiological parameters for glioma grading.

The grading performances of the physiological indices were evaluated for the patients with different glioma grades including grade II (LGG), grade III, grade IV, and high-grade gliomas (HGG, including grade III and grade IV gliomas).

The accuracy, sensitivity, specificity, positive prediction value (PPV), and negative prediction value (NPV) of the physiological indices for glioma grading were determined according to the biopsy results as the gold standard method.

In this study, tumor grade was determined based on the biopsy results and PW-MR imaging data. Kappa index was used to determine the agreement between these grading approaches. The magnitude of the kappa index is ranged from zero to 1. There is a better agreement between the two grading methods when the Kappa coefficient is closer to 1. The kappa coefficient is calculated using Eq. 4.

$$k = \frac{p(a) - p(e)}{1 - p(e)} \tag{4}$$

where $P(a)$ and $P(e)$ are, respectively, the observed and expected agreements between the tumor grades determined using the imaging indices and biopsy results. $P(a)$ and $P(e)$ were calculated using the following equations:

$$P(a) = \frac{\mathrm{TH} + \mathrm{TL}}{\mathrm{TH} + \mathrm{TL} + \mathrm{FH} + \mathrm{FL}} \tag{5}$$

$$P(e) = \frac{\frac{\mathrm{TH} + \mathrm{FL}}{\mathrm{TH} + \mathrm{TL} + \mathrm{FH} + \mathrm{FL}}}{\frac{\mathrm{TH} + \mathrm{FH}}{\mathrm{TH} + \mathrm{TL} + \mathrm{FH} + \mathrm{FL}}} \frac{\mathrm{TL} + \mathrm{FH}}{\mathrm{TH} + \mathrm{TL} + \mathrm{FH} + \mathrm{FL}} \frac{\mathrm{TL} + \mathrm{FL}}{\mathrm{TH} + \mathrm{TL} + \mathrm{FH} + \mathrm{FL}} \tag{6}$$

where TH is the number of patients that were correctly classified using the proposed method as higher-grade glioma (compared with the pathological results), TL is the number of patients that were correctly classified using the proposed method as lower-grade glioma, FH is the number of patients that were wrongly classified using the proposed method as higher-grade glioma, and FL is the number of patients that were wrongly classified using the proposed method as lower-grade glioma.

The grading performances of DCE-MRI-derived physiological indices for glioma grading were also investigated based on a unique classification score including cerebral hemodynamic (rCBV and rCBF), permeability (Ktrans, Kep, etc.), and semi-quantitative (IAUC60 and Peak) indices. In the unique classification score, the weights of the physiological indices were assumed to be the same and equal to 1.

The grading performance of the unique classification score for glioma grading was determined using the method described in Seeger et al. and Matsusue et al. studies [28, 29]. In this method, a grade is assigned to the tumor of each patient. If the patient is classified as a subject with a higher grade glioma, the value of 1 assigned and the value of zero would be assigned to the patient with a lower grade glioma. For each patient, the assigned values are summed. If the achieved value is greater than 3, the patient is classified as a subject with a higher grade of glioma. Otherwise, the patient's tumor would be considered a lower-grade glioma. The classification metrics of this grading system (including kappa coefficient, accuracy, sensitivity, etc.) were also determined using the biopsy results as the gold standard method.

The statistical analyses were performed using SPSS (ver.16.0, SPSS Inc., Chicago, IL) and MATLAB (ver. 2008a, The MathWorks TM, Natick, Massachusetts, United States) softwares.

Results

DCE-MRI data were analyzed using a valid method and the perfusion maps including cerebral hemodynamic (CBV and CBF), permeability (Ktrans, Kep, etc.), and semi-quantitative (IAUC60, Peak, etc.) indices were extracted. The exemplary maps achieved for a 57-year-old woman with glioblastoma multiforme (GBM) are shown in Fig. 1.

The statistical differences of the physiological indices between the different grades of gliomas

The Mann–Whitney U test and independent student T test were used to evaluate the statistical differences of the cerebral hemodynamic (rCBV and rCBF), permeability (Ktrans, Kep, etc.), and semi-quantitative (Peak, IAUC60, etc.) indices between the different grades of gliomas.

The levels of statistical significance for the cerebral hemodynamic (rCBV and rCBF), permeability (Ktrans, Kep, etc.), and semi-quantitative (IAUC60, Peak, etc.) indices between different grades of gliomas are listed in Table 2.

The grading performances of the physiological indices for glioma grading

The optimal thresholds of the cerebral hemodynamic (rCBV and rCBF), permeability (Ktrans, Kep, etc.), and semi-quantitative (Peak, IAUC60, etc.) indices for glioma grading are listed in Tables 3, 4, 5. The accuracy, sensitivity, specificity, PPV, NPV, and Kappa coefficient magnitudes of the physiological indices were also listed in these tables.

The accuracy, sensitivity, specificity, PPV, NPV, and Kappa coefficient magnitudes of the unique grading score for glioma grading are listed in Table 6.

Discussion

Cellularity characteristics and tissue vascularity are two of the main factors that would be considered for glioma grading. Cerebral hemodynamic indices indirectly measure tumor-induced angiogenesis and its microvascular proliferation [19, 22]. Therefore, cerebral hemodynamic indices could be used as bio-imaging markers for tumor grading. In most clinical centers, especially in less developed countries, the cerebral hemodynamic and permeability parameters are currently quantified using a double-dose dynamic imaging procedure including

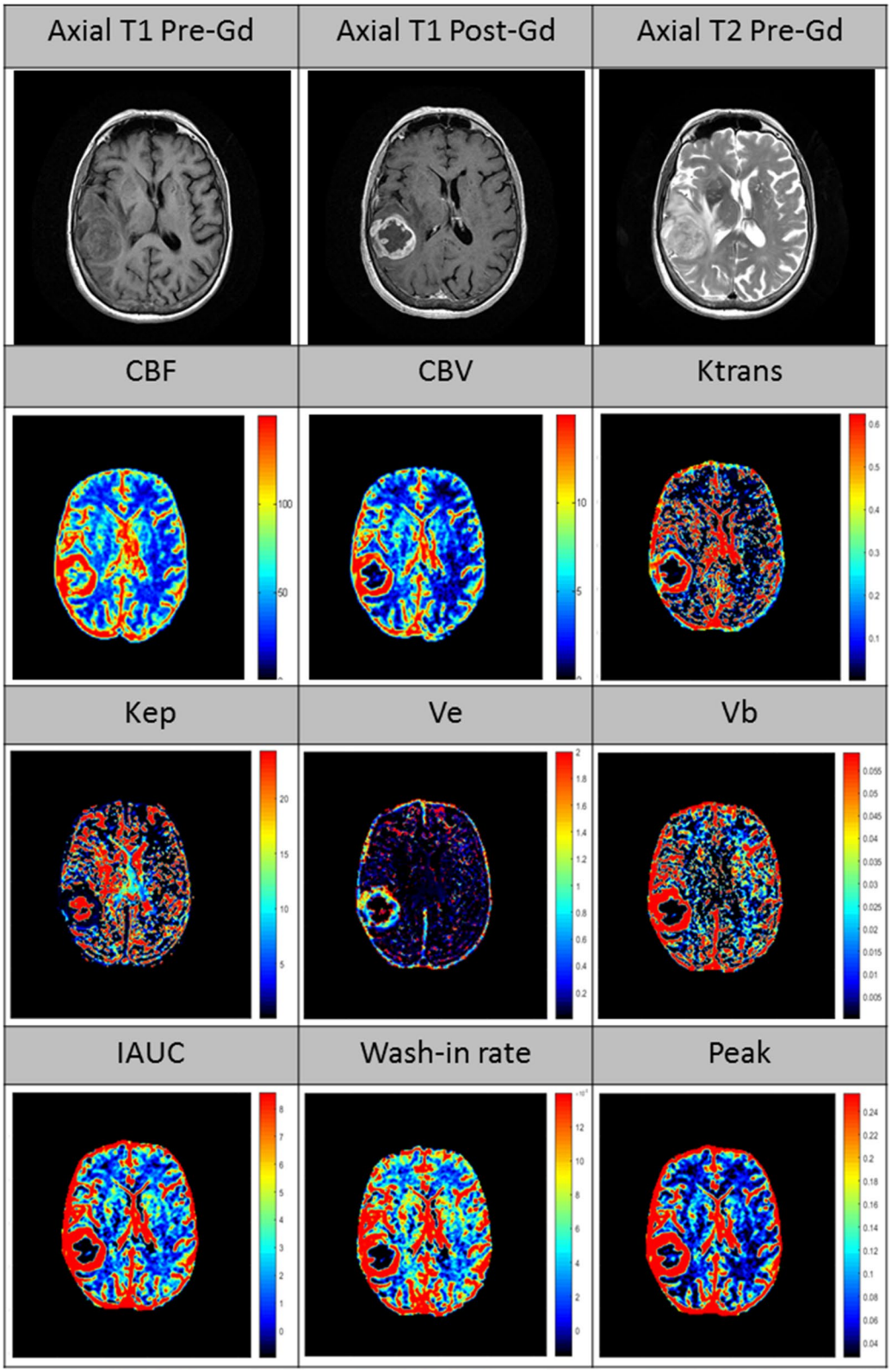

Fig. 1 Exemplary maps achieved for a 57-year-old woman with right temporal *glioblastoma multiforme* (GBM). Axial post-contrast T1-weighted image shows an enhancing lesion in the right temporal lobe. Axial T2-weighted image shows an ill-defined mass with higher signal intensity than the normal brain tissue. The cerebral hemodynamic (CBV and CBF), semi-quantitative ($IAUC_{60}$, Wash-in rate, and Peak), and permeability (Ktrans, Vb, and Ve except for Kep) maps have shown an enhancing lesion in the right temporal lobe. There is a well-discriminated border around the tumor

Table 2 The levels of statistical significance for the cerebral hemodynamic (rCBV and rCBF), permeability (Ktrans, Kep, etc.), and semi-quantitative (IAUC60, Peak, etc.) indices between different grades of gliomas

	GII versus GIII	GII versus GIV	GIII versus GIV	LGG versus HGG
rCBV	0.001	< 0.001	0.004	< 0.001
rCBF	0.027	0.002	0.014	< 0.001
Ktrans (mL/g min)	0.005	< 0.001	0.004	< 0.001
Kep (1/min)	0.040	0.002	0.017	0.001
Vp (mL/g)	0.047	< 0.001	0.001	< 0.001
Ve (mL/g)	0.121	< 0.001	0.070	0.001
$IAUC_{60}$ (mmol Sec /L)	0.006	< 0.001	0.001	< 0.001
Wash-in rate (mmol/L Sec)	0.005	< 0.001	0.013	< 0.001
Peak (mmol/L)	0.007	< 0.001	0.006	< 0.001

Table 3 The accuracy, sensitivity, specificity, PPV, NPV, and Kappa coefficient of cerebral hemodynamic (rCBV and rCBF) indices for differentiation between the different grades of gliomas

		Threshold	Accuracy (%)	Sensitivity (%)	Specificity (%)	PPV (%)	NPV (%)	Kappa Coeff
rCBV	GII versus GIII	2.22	76.92	70	81.25	70	81.25	0.76
	GII versus GIV	3.22	96	100	93.75	90	100	0.96
	GIII versus GIV	4.19	78.95	77.78	80	77.78	80	0.78
	LGG versus HGG	2.80	82.86	84.21	81.25	84.21	81.25	0.82
rCBF	GII versus GIII	2.10	73.08	70	75	63.64	80	0.71
	GII versus GIV	2.53	92	100	87.5	81.82	100	0.92
	GIII versus GIV	2.68	84.21	100	70	75	100	0.83
	LGG versus HGG	2.11	80	84.21	75	80	80	0.79

The discriminative thresholds of cerebral hemodynamic indices were also listed in the first column

Table 4 The accuracy, sensitivity, specificity, PPV, NPV, and Kappa coefficient of permeability (Ktrans, Kep, etc.) indices for differentiation between the different grades of gliomas

		Threshold	Accuracy (%)	Sensitivity (%)	Specificity (%)	PPV (%)	NPV (%)	Kappa Coeff
Ktrans (mL/g min)	GII versus GIII	0.028	76.92	70	81.25	70	81.25	0.76
	GII versus GIV	0.15	100	100	100	100	100	1
	GIII versus GIV	0.2	84.21	88.89	80	80	88.89	0.83
	LGG versus HGG	0.025	82.86	84.21	81.25	84.21	81.25	0.82
Kep (1/min)	GII versus GIII	0.23	53.85	70	43.75	43.75	70	0.51
	GII versus GIV	0.42	76	77.78	75	63.64	85.71	0.75
	GIII versus GIV	0.49	63.16	66.67	60	60	66.67	0.61
	LGG versus HGG	0.29	77.14	78.95	75	78.95	75	0.76
Vp (mL/g)	GII versus GIII	0.045	65.38	80	56.25	53.33	81.82	0.63
	GII versus GIV	0.16	100	100	100	100	100	1
	GIII versus GIV	0.19	84.21	88.89	80	80	88.89	0.83
	LGG versus HGG	0.065	74.29	73.68	75	77.78	70.59	0.73
Ve (mL/g)	GII versus GIII	0.067	57.69	60	56.25	46.15	69.23	0.55
	GII versus GIV	0.28	88	88.89	87.5	80	93.33	0.87
	GIII versus GIV	0.25	78.95	100	60	69.23	100	0.78
	LGG versus HGG	0.15	62.86	68.42	56.25	65	60	0.60

The discriminative thresholds of permeability indices were also listed in the first column

Table 5 The accuracy, sensitivity, specificity, PPV, NPV, and Kappa coefficient of semi-quantitative ($IAUC_{60}$, Peak, etc.) indices for differentiation between the different grades of gliomas

		Threshold	Accuracy (%)	Sensitivity (%)	Specificity (%)	PPV (%)	NPV (%)	Kappa Coeff
$IAUC_{60}$ (mmol Sec/L)	GII versus GIII	3.22	73.08	80	68.75	61.54	84.62	0.71
	GII versus GIV	8.85	100	100	100	100	100	1
	GIII versus GIV	11.47	84.21	100	70	75	100	0.83
	LGG versus HGG	4.49	82.86	73.68	93.75	93.33	75	0.82
Wash-in rate (mmol/L Sec)	GII versus GIII	0.0043	65.38	80	56.25	53.33	81.82	0.63
	GII versus GIV	0.0081	84	77.78	87.5	77.78	87.5	0.83
	GIII versus GIV	0.015	78.95	66.67	90	85.71	75	0.78
	LGG versus HGG	0.0054	62.86	68.42	56.25	65	60	0.60
Peak (mmol/L)	GII versus GIII	0.086	65.38	70	62.5	53.85	76.92	0.63
	GII versus GIV	0.22	96	88.89	100	100	94.12	0.96
	GIII versus GIV	0.34	78.95	88.89	70	72.73	87.5	0.78
	LGG versus HGG	0.110	85.71	84.21	87.5	88.89	82.35	0.85

The discriminative thresholds of semi-quantitative indices were also listed in the first column

Table 6 The accuracy, sensitivity, specificity, PPV, NPV, and Kappa coefficient of the unique classification score (including cerebral hemodynamic, permeability, and semi-quantitative indices) for differentiation between the different grades of gliomas

	Accuracy (%)	Sensitivity (%)	Specificity (%)	PPV (%)	NPV (%)	Kappa Coeff
GII versus GIII	84.62	90	81.25	75	92.86	0.84
GII versus GIV	100	100	100	100	100	1
GIII versus GIV	94.74	100	90	90	100	0.94
LGG versus HGG	91.43	89.47	93.75	94.44	88.24	0.91

DSC-MRI and DCE-MRI techniques. In this study, an optimized DCE-MRI paradigm was used that could simultaneously present both cerebral hemodynamic and permeability parameters using a single dose acquisition. To evaluate the clinical significances of the parameters quantified using this method, the achieved magnitudes for different glioma grades and their performances for glioma grading are compared with reported values.

For high-grade gliomas, high CBV and CBF areas are more expected in cerebral hemodynamic maps [30, 31]. In our study, higher cerebral hemodynamic magnitudes were quantified for the high-grade gliomas (rCBV: 5.28 ± 3.02 vs. 2.03 ± 0.78; and rCBF: 3.57 ± 1.68 vs. 1.94 ± 0.97) that reflects higher angiogenic activity for high-grade gliomas. These parameters could indicate the metabolism and vascularity characteristics of the tumor [31].

In our study, the mean rCBVs for grade II (LGG), grade III, grade IV, and high-grade gliomas were 2.03 ± 0.78, 3.61 ± 1.64, 7.14 ± 3.19, and 5.28 ± 3.02, respectively. The mean rCBFs for grade II (LGG), grade III, grade IV, and high-grade gliomas were, respectively, quantified as 1.94 ± 0.97, 2.67 ± 0.96, 4.57 ± 1.77, and 3.57 ± 1.68. In previous studies, different rCBV and rCBF values were reported for low- and high-grade gliomas. rCBV magnitudes ranged from 0.89 to 3.94 and 2.15 to 9.84 for low- and high-grade gliomas, respectively. The reported rCBF magnitudes for low- and high-grade gliomas, respectively, ranged from 0.85 to 3.79 and 2.55 to 8.26. In Stefano et al. study [27], rCBV values were calculated in three different compartments including the contrast-enhanced area, the non-enhancing tumor, and the high perfusion area on the CBV maps for twenty-one patients with grade III and IV gliomas. The rCBV values for grades III and IV were 3.78 ± 1.70 and 7.51 ± 3.84, respectively. In Saini et al. [32] study, the mean rCBVs for grades II, III, and IV gliomas were, respectively, reported as 1.84 ± 0.57, 4.16 ± 1.49, and 6.09 ± 3.04. Our results were similar to those of these studies.

In the next step, rCBF values quantified for different glioma grades are compared with the reported magnitudes in other studies. In Falk et al. study [33], the grades II and III gliomas were investigated using DSC- and DCE-MR imagings. The mean rCBFs for grades II and III gliomas were 1.66 ± 0.99 and 2.53 ± 1.88, respectively. The glioma grading based on perfusion parameters was also evaluated by Server et al. [34]. The mean rCBFs for grades II, III, and IV were, respectively, reported as 2.87 ± 2.14,

5.35 ± 2.04, and 5.34 ± 1.93. There was no significant difference between grade III and IV gliomas. For the relative hemodynamic indices, there were significant differences between the different grades of gliomas. Our findings, in agreement with these studies, indicate the statistically significant differences in rCBV and rCBF values between grades II (LGG), grade III, grade IV, and high-grade gliomas ($P < 0.027$).

According to the promising observations for the perfusion indices quantified using DCE-MRI data in comparison with the reported studies, in the next step, the classification performances of these parameters are evaluated. Our best rCBF and rCBV thresholds for differentiating between low- and high-grade gliomas were 2.11 (accuracy = 80%, sensitivity = 84.21%, and specificity = 75%) and 2.80 (accuracy of 82.86%, sensitivity = 84.21%, and specificity = 81.25%), respectively. In Ma et al. study [35], ASL and DSC-MR imagings were used for preoperative glioma grading. In this study, twenty-seven low-grade gliomas and twenty-three high-grade gliomas were investigated. For the ASL method, rCBF cut-off of 2.24 with sensitivity = 83.2%, specificity = 77.7%, and AUC = 0.866 was suggested as the optimal threshold. In the DSC-MRI method, the best rCBF cut-off was 1.85 (sensitivity = 91.3%, specificity = 63.9%, and AUC = 0.758). In Caulo et al. study [36], the glioma grading was performed using a multimodal MRI method. For the rCBV cut-off value of 2.59 in contrast-enhanced regions, the sensitivity and specificity values were 80% and 91%, respectively. In a similar study [37], the rCBV index was also used for glioma grading in 160 patients. For the rCBV threshold of 2.97, the sensitivity, specificity, PPV, and NPV were reported as 72.5%, 87.5%, 94.6%, and 51.5%, respectively.

Our cut-off magnitudes for DCE-MRI-derived cerebral hemodynamic indices and their grading performances to discriminate low- and high-grade gliomas were similar to the results of the reported studies. Therefore, it could be concluded that relative cerebral hemodynamic parameters quantified using the DCE-MRI method have acceptable accuracies for differentiating between low- and high-grade gliomas.

The best rCBV thresholds reported for differentiating between grade II and III gliomas and between grade III and IV gliomas were, respectively, 2.4 (sensitivity = 100% and specificity = 92%) and 3.92 (sensitivity = 81% and specificity = 58%) [37]. There is good agreement between our threshold magnitudes and their grading performances with the values reported in the literature. The observed compliances between the magnitudes of perfusion indices and their classification performances for glioma grading in our study and those of the reported studies emphasize the clinical efficiencies of the DCE-MRI-derived perfusion parameters for glioma grading. Therefore, the perfusion indices quantified using DCE-MRI data could be promising and efficient classifier factors for glioma grading.

In medical imaging centers, the DCE-MRI method is routinely used to investigate the permeability characteristics of the tissues. In the second part of our study, the permeability indices were quantified for different glioma grades and the classification performances of these permeability indices were evaluated for glioma grading. Higher vascular permeability magnitudes (Ktrans: 0.37 ± 0.4 vs. 0.017 ± 0.02, and Kep: 0.55 ± 0.36 vs. 0.22 ± 0.17) were measured for the high-grade gliomas in agreement with the other studies. Higher proportions of immature blood vessels with high permeability characteristics would result due to increased angiogenesis in high-grade gliomas [32, 38]. Vascular endothelial permeability in brain tumors reflects valuable information about the blood–brain barrier defects, the characteristics of neoangiogenesis, and vascular morphology for tumoral tissues. Hence, the permeability indices could play an important role in tumor identification, in addition to tumor grading [28, 39, 40].

In Li et al. study [4], the classification performances of DCE-MRI and SWI methods were investigated for glioma grading. In this study, Ktrans and Ve parameters were evaluated for 32 patients with different grades of gliomas. The mean Ktrans values for grade II, III, and IV gliomas were 0.026 ± 0.019, 0.096 ± 0.063 min^{-1}, and 135 ± 0.068 min^{-1}, respectively. For grade II, III, and IV gliomas, the mean Ve values were, respectively, reported as 0.121 ± 0.13, 0.483 ± 0.225, and 0.525 ± 0.18. In Ludemann et al. study [41], permeability parameters were also quantified for forty-one gliomas, six meningiomas, and eight metastases. The mean Ktrans values for grade II, III, and IV gliomas were 1.584 min^{-1}, 1.338 min^{-1}, and 1.821 min^{-1}, respectively. For grade II, III, and IV gliomas, the mean Ve values were, respectively, reported as 18.03, 25.26, and 22.41.

There are considerable differences between the mean permeability magnitudes reported by previous studies. In these studies, different grading cut-off values were also proposed [1, 4, 18, 41–43]. These huge discrepancies may be related to the differences in pulse sequences, pharmacokinetic models, dynamic scanning times, and arterial input function (AIF) selection procedures used in the studies[43, 44].

There were statistically significant differences in Ktrans and Kep parameters between different grades of gliomas, which was consistent with our results. In Li et al. and Zhao et al. studies [4, 42], similar to our findings, there were statistically significant differences in Ve between grade II and IV gliomas and between LGG and HGG

groups. There was no significant difference between grade III and IV gliomas, which was also observed in our findings. These observations indicated that the permeability indices can complement histopathology results for tumor grading by providing valuable information about tumor vascular permeability.

In studies like that of Santarosa et al. [18], the double-dose acquisition was used to quantify the rCBV, Vp, and Ktrans parameters. But, in our study, a more comprehensive collection of the physiological indices was measured using a single-dose DCE-MRI acquisition. On the other hand, DCE-MRI is not affected by susceptibility artifacts and has a higher spatial resolution than the conventional DSC-MRI [18, 45]. Therefore, in addition to financial and patient safety issues, much better grading parameters could be achieved using DCE-MRI-derived physiological indices.

In our study, there were significant differences in DCE-MRI-derived physiological indices (except for Ve) between the different grades of gliomas, and the glioma grades were accurately classified using these parameters. In discriminating the glioma grades, the unique classification score had the best grading performance compared to each physiological index separately. Even though, each of the physiological indices provides useful biological and physiological information about the lesions. For glioma grading based on DCE-MRI-derived physiological indices, a unique classification score consisting of all physiological indices is proposed. The cerebral hemodynamic and permeability indices quantified using the single-dose DCE-MRI could also help to determine the lesion characteristics as a non-invasive method.

Limitations

This study had some limitations. First, this is a single-center study and participants were primarily local residents. These limitations restrict the generalizability of the results for other countries. External validation of the proposed paradigm merits future investigations using bigger and multicenter databases.

Second, the DCE-MRI-derived cerebral hemodynamic and permeability indices of different glioma grades and the grading performance of these physiological indices were only evaluated for glioma grading and could not be readily translated to other tumors.

Conclusions

In this study, the grading performances of DCE-MRI-derived physiological indices were evaluated for glioma grading. A more comprehensive collection of the physiological parameters including the cerebral hemodynamic and permeability indices could be achieved using a single-dose DCE-MRI approach. The cerebral hemodynamic and permeability indices quantified using the DCE-MRI could determine glioma grades with an acceptable agreement with histopathological results. For glioma grading based on DCE-MRI-derived physiological indices, a unique classification score consisting of all physiological indices is proposed. The cerebral hemodynamic and permeability indices quantified using DCE-MRI could also help to determine the lesion characteristics as a non-invasive method.

Abbreviations

CBV	Cerebral blood volume
CBF	Cerebral blood flow
rCBV	Relative cerebral blood volume
rCBF	Relative cerebral blood flow
MRI	Magnetic resonance imaging
DCE-MRI	Dynamic contrast-enhanced MRI
DSC-MRI	Dynamic susceptibility contrast MRI
PW-MRI	Perfusion weighted-MRI
HGG	High-grade glioma
LGG	Low-grade glioma
WHO	World Health Organization
IAUC	Initial area under the curve
PPV	Positive prediction value
NPV	Negative prediction value
ROI	Region of interest
AIF	Arterial input function
GBM	Glioblastoma multiforme

Acknowledgements

Authors would like to thank the research affair of Erbil Polytechnic University, Medical Imaging Center of Erbil Teaching Hospital (Erbil), and participants in the study.

Author contributions

AIA contributed to Conceptualization; Data gathering; Formal analysis; Investigation; Project administration; Funding acquisition; Methodology; Resources; Supervision; Writing, review, and editing—original draft.
AIA read and approved the final manuscript.

Funding

This research has been supported by Erbil Polytechnic University.

Availability of data and materials

All data generated and analyzed during the current study are not publicly available but are available from the corresponding author on reasonable request and Erbil Polytechnic University' approval.

Declarations

Ethics approval and consent to participate

This article is extracted from a research project supported by Erbil Polytechnic University and all experimental protocols were approved by the ethical committee of Erbil Polytechnic University. All methods of the study were performed in accordance with the relevant guidelines and regulations of the ethical committee of Erbil Polytechnic University. Participation was voluntary and informed consent was obtained from all subjects and/or their legal guardians. Participants had the right to withdraw from the study at any time.

Consent for publication

Not applicable.

Competing interests
The authors declare that they have no competing interests.

Received: 21 September 2023 Accepted: 30 December 2023
Published online: 16 February 2024

References

1. Jia Z, Geng D, Xie T, Zhang J, Liu Y (2012) Quantitative analysis of neovascular permeability in glioma by dynamic contrast-enhanced MR imaging. J Clin Neurosci 19(6):820–823
2. Tate MC, Aghi MK (2009) Biology of angiogenesis and invasion in glioma. Neurotherapeutics 6(3):447–457
3. Pauliah M, Saxena V, Haris M, Husain N, Rathore RKS, Gupta RK (2007) Improved T 1-weighted dynamic contrast-enhanced MRI to probe microvascularity and heterogeneity of human glioma. Magn Reson Imaging 25(9):1292–1299
4. Li X, Zhu Y, Kang H et al (2015) Glioma grading by microvascular permeability parameters derived from dynamic contrast-enhanced MRI and intratumoral susceptibility signal on susceptibility weighted imaging. Cancer Imaging 15(1):4
5. Lemasson B, Chenevert TL, Lawrence TS et al (2013) Impact of perfusion map analysis on early survival prediction accuracy in glioma patients. Transl Oncol 6(6):766–774
6. Gupta A, Dwivedi T (2017) A simplified overview of World Health Organization classification update of central nervous system tumors 2016. J Neurosci Rural Pract 8(04):629–641
7. Diamandis P, Aldape K (2018) World Health Organization 2016 classification of central nervous system tumors. Neurol Clin 36(3):439–447
8. Jiri B Jr, Jiri B Sr, Carter B, Chen CC, Ng K, Kesari S (2011) Key principles in glioblastoma therapy. INTECH Open Access Publisher
9. Awasthi R, Rathore RK, Soni P et al (2012) Discriminant analysis to classify glioma grading using dynamic contrast-enhanced MRI and immunohistochemical markers. Neuroradiology 54(3):205–213
10. Daumas-Duport C, Scheithauer B, O'Fallon J, Kelly P (1988) Grading of astrocytomas: a simple and reproducible method. Cancer 62(10):2152–2165
11. Hakyemez B, Erdogan C, Ercan I, Ergin N, Uysal S, Atahan S (2005) High-grade and low-grade gliomas: differentiation by using perfusion MR imaging. Clin Radiol 60(4):493–502
12. Patankar TF, Haroon HA, Mills SJ et al (2005) Is volume transfer coefficient (Ktrans) related to histologic grade in human gliomas? AJNR Am J Neuroradiol 26(10):2455–2465
13. Lüdemann L, Grieger W, Wurm R, Budzisch M, Hamm B, Zimmer C (2001) Comparison of dynamic contrast-enhanced MRI with WHO tumor grading for gliomas. Eur Radiol 11(7):1231–1241
14. Cebeci H, Aydin O, Ozturk-Isik E et al (2014) Assesment of perfusion in glial tumors with arterial spin labeling; comparison with dynamic susceptibility contrast method. Eur J Radiol 83(10):1914–1919
15. Al-Okaili RN, Krejza J, Wang S, Woo JH, Melhem ER (2006) Advanced MR imaging techniques in the diagnosis of intraaxial brain tumors in adults. Radiographics 26(suppl_1):S173–S189
16. Jiang J, Zhao L, Zhang Y et al (2014) Comparative analysis of arterial spin labeling and dynamic susceptibility contrast perfusion imaging for quantitative perfusion measurements of brain tumors. Int J Clin Exp Pathol 7(6):2790
17. Gagner JP, Law M, Fischer I, Newcomb EW, Zagzag D (2005) Angiogenesis in gliomas: imaging and experimental therapeutics. Brain Pathol 15(4):342–363
18. Santarosa C, Castellano A, Conte GM et al (2016) Dynamic contrast-enhanced and dynamic susceptibility contrast perfusion MR imaging for glioma grading: preliminary comparison of vessel compartment and permeability parameters using hotspot and histogram analysis. Eur J Radiol 85(6):1147–1156
19. Barajas RF Jr, Cha S (2014) Benefits of dynamic susceptibility-weighted contrast-enhanced perfusion MRI for glioma diagnosis and therapy. CNS Oncol 3(6):407–419
20. Sourbron S, Ingrisch M, Siefert A, Reiser M, Herrmann K (2009) Quantification of cerebral blood flow, cerebral blood volume, and blood–brain-barrier leakage with DCE-MRI. Magn Reson Med 62(1):205–217
21. Singh A, Haris M, Rathore D et al (2007) Quantification of physiological and hemodynamic indices using T1 dynamic contrast-enhanced MRI in intracranial mass lesions. J Magn Reson Imaging 26(4):871–880
22. Zakariaee SS, Oghabian MA, Firouznia K, Sharifi G, Arbabi F, Samiei F (2018) Assessment of the agreement between the perfusion indices quantified using dynamic contrast enhanced and dynamic susceptibility contrast perfusion magnetic resonance imagings. J Clin Imaging Sci 8(1):1–9
23. Nielsen T, Wittenborn T, Horsman MR (2012) Dynamic contrast-enhanced magnetic resonance imaging (DCE-MRI) in preclinical studies of antivascular treatments. Pharmaceutics 4(4):563–589
24. Zhang W, Chen HJ, Wang ZJ, Huang W, Zhang LJ (2016) Dynamic contrast enhanced MR imaging for evaluation of angiogenesis of hepatocellular nodules in liver cirrhosis in N-nitrosodiethylamine induced rat model. Eur Radiol, pp 1–9
25. Zhao J, Yang Z-y, Luo B-n, Yang J-y, Chu J-p (2015) Quantitative evaluation of diffusion and dynamic contrast-enhanced MR in tumor parenchyma and peritumoral area for distinction of brain tumors. PLoS ONE 10(9):e0138573
26. Larsson HB, Courivaud F, Rostrup E, Hansen AE (2009) Measurement of brain perfusion, blood volume, and blood-brain barrier permeability, using dynamic contrast-enhanced T1-weighted MRI at 3 tesla. Magn Reson Med 62(5):1270–1281
27. Di Stefano AL, Bergsland N, Berzero G, et al (2014) Facing contrast-enhancing gliomas: perfusion MRI in grade III and grade IV gliomas according to tumor area. BioMed Res Int
28. Seeger A, Braun C, Skardelly M et al (2013) Comparison of three different MR perfusion techniques and MR spectroscopy for multiparametric assessment in distinguishing recurrent high-grade gliomas from stable disease. Acad Radiol 20(12):1557–1565
29. Matsusue E, Fink JR, Rockhill JK, Ogawa T, Maravilla KR (2010) Distinction between glioma progression and post-radiation change by combined physiologic MR imaging. Neuroradiology 52(4):297–306
30. Calli C, Kitis O, Yunten N, Yurtseven T, Islekel S, Akalin T (2006) Perfusion and diffusion MR imaging in enhancing malignant cerebral tumors. Eur J Radiol 58(3):394–403
31. Rizzo L, Crasto SG, Moruno PG et al (2009) Role of diffusion-and perfusion-weighted MR imaging for brain tumour characterisation. Radiol Med 114(4):645–659
32. Saini J, Gupta PK, Sahoo P, et al (2017) Differentiation of grade II/III and grade IV glioma by combining "T1 contrast-enhanced brain perfusion imaging" and susceptibility-weighted quantitative imaging. Neuroradiology, pp. 1–8
33. Falk A, Fahlström M, Rostrup E et al (2014) Discrimination between glioma grades II and III in suspected low-grade gliomas using dynamic contrast-enhanced and dynamic susceptibility contrast perfusion MR imaging: a histogram analysis approach. Neuroradiology 56(12):1031–1038
34. Server A, Graff BA, Orheim TED et al (2011) Measurements of diagnostic examination performance and correlation analysis using microvascular leakage, cerebral blood volume, and blood flow derived from 3T dynamic susceptibility-weighted contrast-enhanced perfusion MR imaging in glial tumor grading. Neuroradiology 53(6):435–447
35. Ma H, Wang Z, Xu K et al (2017) Three-dimensional arterial spin labeling imaging and dynamic susceptibility contrast perfusion-weighted imaging value in diagnosing glioma grade prior to surgery. Exp Ther Med 13(6):2691–2698
36. Caulo M, Panara V, Tortora D et al (2014) Data-driven grading of brain gliomas: a multiparametric MR imaging study. Radiology 272(2):494–503
37. Law M, Yang S, Wang H et al (2003) Glioma grading: sensitivity, specificity, and predictive values of perfusion MR imaging and proton MR spectroscopic imaging compared with conventional MR imaging. AJNR Am J Neuroradiol 24(10):1989–1998
38. Bangiyev L, Espagnet MCR, Young R et al (eds) (2014) Adult brain tumor imaging: state of the art. Elsevier, Semin Roentgenol
39. Jain R (2013) Measurements of tumor vascular leakiness using DCE in brain tumors: clinical applications. NMR Biomed 26(8):1042–1049
40. Law M (2009) Advanced imaging techniques in brain tumors. Cancer Imaging. https://doi.org/10.1102/1470-7330.2009.9002

41. Lüdemann L, Grieger W, Wurm R, Wust P, Zimmer C (2005) Quantitative measurement of leakage volume and permeability in gliomas, meningiomas and brain metastases with dynamic contrast-enhanced MRI. Magn Reson Imaging 23(8):833–841
42. Zhao M, Guo LL, Huang N et al (2017) Quantitative analysis of permeability for glioma grading using dynamic contrast-enhanced magnetic resonance imaging. Oncol Lett 14(5):5418–5426
43. Piyapittayanan S, Segsarnviriya C, Ngamsombat C et al (2017) Comparison between dynamic contrast-enhanced MRI and dynamic susceptibility contrast MRI in glioma grading. Siriraj Med J 69(6):369–376
44. Jackson A (2004) Analysis of dynamic contrast enhanced MRI. Br J Radiol 77(suppl_2):S154–S166
45. Larsson HB, Hansen AE, Berg HK, Rostrup E, Haraldseth O (2008) Dynamic contrast-enhanced quantitative perfusion measurement of the brain using T1-weighted MRI at 3T. J Magn Reson Imaging 27(4):754–762

Publisher's Note